ISSN 0010-5082, Combustion, Explosion, and Shock Waves, 2021, Vol. 57, No. 4, pp. 385–397. © Pleiades Publishing, Ltd., 2021.

Synthesis of Ceramic and Composite Materials Using a Combination of Self-Propagating High-Temperature Synthesis and Spark Plasma Sintering (Review)

T. M. Vidyuk[a,b], M. A. Korchagin[a,c], D. V. Dudina[a,c,d], and B. B. Bokhonov[a]

UDC 541.124

Published in *Fizika Goreniya i Vzryva*, Vol. 57, No. 4, pp. 3–17, July–August, 2021.
Original article submitted July 16, 2020; revision submitted September 7, 2020; accepted for publication October 10, 2020.

Abstract: This review deals with the potential of combining self-propagating high-temperature synthesis (SHS) and spark plasma sintering (SPS) for obtaining single-phase ceramic materials and ceramic and metal matrix composites. The materials discussed in this review contain compounds produced by the SHS process: carbides, borides, and silicides of metals and intermetallics. Factors in the structure formation of materials obtained by sintering of SHS products and the influence of SPS conditions on the characteristics of the materials (relative density and grain size) are analyzed. Advantages of combining the SHS and SPS techniques, including the possibility of additional processing of SHS products (grinding and adding components) to modify the composition and properties of materials are discussed.

Keywords: self-propagating high-temperature synthesis, spark plasma sintering, reactive sintering, ceramic materials, composite materials, microstructure, morphology, grain growth, grain boundaries, heating rate, mechanical properties.

DOI: 10.1134/S0010508221040018

INTRODUCTION

Self-propagating high-temperature synthesis (SHS) is a promising direction in the development of chemistry and materials science. This synthesis technique is based on the ignitability of powder materials under local heating, after which the combustion front self-propagates in the powder sample due to heat transfer, thus initiating further reaction.

SHS is an attractive method from a technological point of view due to its fast process. During SHS, the heating rates of initial components can reach 10^3–10^6 deg/s, and the characteristic reaction time is 10^{-3} to 10^{-1} s [1]. The concept of primary and secondary structure formation of SHS products was proposed by Merzhanov [2, 3]. The processes occurring in the SHS reaction front are called primary structure formation. The primary microstructure of SHS products is characterized by a small grain size and the presence of melt. Secondary structure formation involves grain growth, ordering of the crystal structure, and the establishment of a more uniform distribution of elements in the products. The sample cooling time usually ranges from a second to several minutes.

Studies of SHS processes are widely presented in the literature. Traditionally, SHS is used to obtain materials based on refractory metal–nonmetal compounds such as carbides, borides, silicides, and nitrides [1, 4, 5].

[a] Institute of Solid State Chemistry and Mechanochemistry, Siberian Branch, Russian Academy of Sciences, Novosibirsk, 630128 Russia.
[b] Khristianovich Institute of Theoretical and Applied Mechanics, Siberian Branch, Russian Academy of Sciences, Novosibirsk, 630090 Russia; vidyuk@itam.nsc.ru.
[c] Novosibirsk State Technical University, Novosibirsk, 630073 Russia.
[d] Lavrentyev Institute of Hydrodynamics, Siberian Branch, Russian Academy of Sciences, Novosibirsk, 630090 Russia.

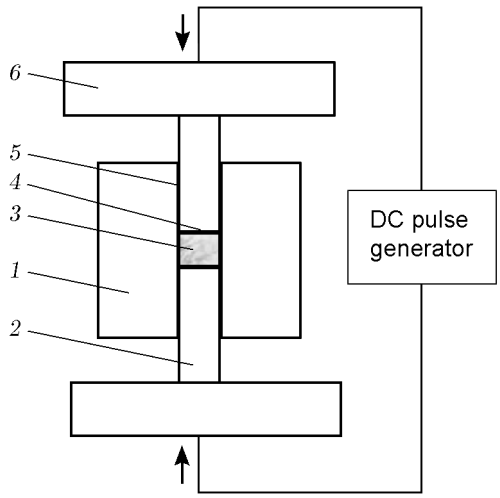

Fig. 1. SPS principle and equipment used: (*1*) graphite die; (*2*) graphite punches; (*3*) sample; (*4*, *5*) protective foil; (*6*) graphite discs.

SHS is also used for the synthesis of intermetallic compounds [6–8]. A great number of papers are devoted to the fabrication of composite powders in which refractory ceramic particles are distributed in a metal matrix [9–12]. SHS products are powders or porous sintered materials with low mechanical strength. Therefore, after the synthesis, the products require crushing and grinding. To obtain a nonporous bulk material, it is necessary to consolidate the synthesis product. This can be done using various methods: hot pressing, microwave sintering or sintering by electric current.

There are various methods for electric current sintering [13]. The best-known and most widely used method in laboratory practice is spark plasma sintering (SPS), in which DC pulses are passed through a sample throughout the entire period of sintering. It is common to use low voltage (less than 10 V). The SPS equipment is shown schematically in Fig. 1.

Passing an electric current pulse through a sample leads to electrical discharges at the contacts between particles, resulting in the formation of local high-temperature regions. During repeated pulses, high-temperature regions move in the sample, providing uniform sintering throughout the volume. Sintering in the die under pressure provides higher density and improved mechanical properties of the sintered material compared to free sintering. Using this method reduces the sintering time to several minutes. Local heating of contacts between particles can lead to initiation of chemical reactions during sintering of mixtures of powders of dissimilar materials. Currently, SPS is widely used to obtain ceramic, metal, and composite materials [14]. If the sintered material is conductive, electric current passes directly through the sample during sintering. If the sintered material does not conduct electric current, it is heated from the conductive punches and die. The SPS technique is also employed for reactive sintering, in which the compaction of the powder sample is accompanied by the synthesis of new phases.

SPS has advantages over other methods of powder consolidation, such as traditional reactive sintering and hot pressing. First, the use of electric current pulses significantly increases the sample heating rate, which depends on the resistance of the sintered material and the die diameter and can reach 1000°C/min [15]. Second, sintering is possible at lower temperatures and short holding times. Thus, shortening the time of temperature holding during sintering does not provide significant growth of material grains [16]. In sintered materials, metastable phases and high concentrations of crystal lattice defects can be preserved. These features make it possible to obtain materials with improved mechanical characteristics.

The stages of the SPS process are described by Holland et al. [17]. In the first (initial) stage of sintering, a neck forms at the contact between particles and its growth begins. In the initial stage, recrystallization is absent and only a slight shrinkage of the material occurs. This stage is dominated by surface diffusion; evaporation and condensation processes also take place. The question of whether plasma forms during SPS remains controversial [18, 19]. During sintering at the initial stage, the temperature increases at particle contact sites due to the higher electrical resistance of the contact area, which can lead to local melting of the material. Heating of particles at the contacts provides uniform sintering over the entire volume of the sample. There is evidence that during sintering, oxide films detach from the surface of the particles, which can lead to more intense grain-boundary diffusion [20]. At the second (intermediate) stage of sintering, pore spheroidization occurs [17]. The porosity of the sample decreases due to the growth of necks between particles. The greatest contribution to mass transfer at the intermediate stage comes from grain-boundary and volume diffusions. At the end of the intermediate stage, grain growth is observed. When all the pores in the material become closed, the intermediate sintering stage is considered complete. The third (final) sintering stage is characterized by grain growth and a decrease in residual porosity. Evaporation and condensation are also present at this stage. Pore size reduction at the final sintering stage is mainly due to grain-boundary and volume diffusions.

To obtain consolidated composite and ceramic materials, it is of interest to combine the SHS and SPS techniques. SHS products have a high density of struc-

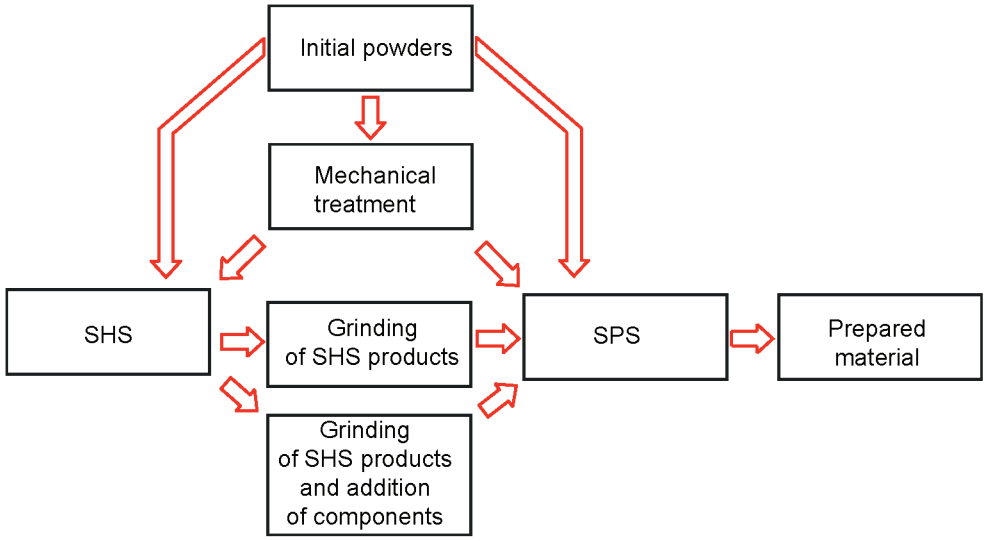

Fig. 2. Sequence of operations for obtaining composite and ceramic materials by the reactive SPS method and by the method of SPS of SHS products.

tural defects and a small grain size. SPS as a rapid method for obtaining bulk materials allows preserving the phase composition and structural features of the powders being sintered. SPS of SHS produced powders makes it possible to fabricate bulk materials with low residual porosity and improved mechanical properties.

The purpose of this review is to analyze the potential of combining SHS and SPS for obtaining ceramic materials and ceramic and metal matrix composites. Studies in which SHS and SPS were combined to obtain compact materials and studies on the reactive sintering of powders are considered.

Figure 2 shows various methods for obtaining bulk materials, including reactive SPS and sintering of SHS products. In most studies, the synthesis temperature was reduced by mechanical activation (treatment) of initial powders. Mechanical treatment is an important stage in the fabrication of ceramic and composite materials with controlled microstructure. SHS products usually require grinding. During grinding, additional components can be added to SHS products (see Fig. 2). It should be noted that the mechanical treatment of powders is optional, and, in some cases, SHS and reactive SPS are carried out using mixtures of powder reactants obtained by traditional mixing.

COMBINING SHS AND SPS TECHNIQUES

A comparison of reactive and nonreactive SPS for obtaining single-phase ceramic materials and composites with a ceramic matrix is presented in [21]. The possibilities of obtaining ultra-high-temperature ceramics by combining SHS and SPS techniques are analyzed. Attention is focused on the synthesis of hafnium diboride (HfB_2), tantalum diboride (TaB_2), and zirconium diboride (ZrB_2). It is noted [22, 23] that in obtaining single-phase ceramics, a higher relative density of the material (up to 100%) can be achieved by using reactive sintering, where the synthesis of diborides occurs directly during heating of the reaction mixture in the SPS setup. In the cited studies, a two-stage procedure of applying mechanical pressure was used: the pressure was increased after the start of the synthesis. In exothermic reactions accompanied by the release of a significant amount of heat, the temperatures of the sample and the dies increase sharply, making it possible to determine the beginning of the synthesis and control the mechanical pressure during sintering. At the same time, during the synthesis of ZrB_2–SiC and TaB_2–SiC ceramic composites, SPS of SHS products made it possible to obtain a denser material than reactive sintering. The relative density of sintered materials exceeded 99% of the theoretical value [24]. It has been found that to obtain a dense material by sintering of composite SHS products, milder conditions (lower temperature and shorter holding time) are required than in the case of reactive sintering of the same compositions [24, 25].

It is noted [21] that SHS products have a high density of structural defects and a small grain size. These structural features contribute to the production of bulk composites with a high relative density by SPS. The

high heating and cooling rates of the sample during SHS lead to the formation of defects, which during subsequent sintering, provide effective compaction of the material. In addition, if different ceramic components are simultaneously formed during SHS, then diffusion processes at the interfaces can lead to the formation of stronger bonds, which also contributes to the production of materials with low residual porosity during subsequent sintering.

SYNTHESIS OF SINGLE-PHASE CERAMIC MATERIALS

The number of studies of the sintering of SHS products continues to increase. Some of them have shown differences in the structural characteristics of single-phase ceramic materials obtained by reactive and nonreactive SPS and the difference in their relative densities. A comparative study of the microstructure and mechanical properties of zirconium diboride (ZrB_2) obtained by reactive SPS and the material obtained by SPS of the SHS powder of zirconium diboride (SHS product) was performed in [26]. In both cases, the mixture of the initial boron powders and zirconium was pre-treated in a ball mill to activate the synthesis.

It is known that mechanical activation significantly changes the combustion temperature and rate, leading to changes in the structure and properties of synthesis products [27–29]. Traditional SHS compositions have a specific dependence of the reaction rate on temperature. When using typical powder mixtures with reactant particles tens or hundreds of micrometers in size, only slow solid-state reactions are observed in them up to the melting point of one of the reactants or the formation of a eutectic melt. However, the formation of the melt is accompanied by a sharp (3–4 orders of magnitude) increase in the reaction rate. Only in this case is it possible to carry out self-propagating reaction with layer-by-layer propagation of the synthesis wave or in the thermal explosion mode [1]. Pre-activation of reaction mixtures leads to a significant decrease in the ignition temperature and the maximum temperature of the subsequent exothermic reaction. In addition, in some low-calorific-value compositions, it is possible to achieve solid-state combustion or thermal explosion [30–32]. These effects are due to the fact that activation results in mechanocomposites, in which the reactants are dispersed to nanometer sizes, the area of their contact increases manifold, and there is a high concentration of nonequilibrium defects and internal stresses. In conventional powder mixtures, the contact area between particles is 10^{-4} to 10^{-7} of the total surface of the particles. It can be assumed that in the mechanocomposites formed, the contact area of reactants increases to almost one. In the early stages of activation of the initial reaction mixture, there is destruction of oxide layers and adsorbed films on powder particles which are serious diffusion barriers to the start of interaction. It is known that part of the energy delivered during activation (≈5–10%) is accumulated by the sample. This produces a high concentration of nonequilibrium defects and internal stress in the sample. Thus, the transition from the initial powder mixture of reactants to mechanocomposites should affect the main parameters of the subsequent self-propagating reaction. It has been found that preactivation leads to an increase in the combustion rate of SHS compositions. In addition, it allows one to expand the concentration limits of SHS, use compositions for synthesis that do not burn in the case of powder mixtures, and to avoid the need to press the initial samples.

In [26], the formation reaction of ZrB_2 in SHS proceeds completely, and further sintering is used to obtain nonporous material. Relative density over 96% is achieved by sintering the SHS product at a temperature of 1900°C and a pressure of 50 MPa for 20 min. The obtained relative density is not inferior to the values for ZrB_2 synthesized by reactive SPS at the same temperature and pressure [33]. It should be noted that there are significant differences in the grain size of ZrB_2 synthesized by these methods. The average grain size of ZrB_2 ceramic obtained by SHS–SPS does not exceed 20 μm, while in the case of reactive SPS, it is 50 μm.

In [26], tantalum diboride (TaB_2) with a relative density of ≈ 94% was obtained by combining SHS and SPS techniques, and the SHS product was subjected to grinding. Higher relative density of TaB_2 was not achieved even at a pressure of 60 MPa. In this case, in comparison with ZrB_2, the microstructure of TaB_2 samples consisted of smaller grains, which was attributed by the authors of [26],to the difference in the size of aggregates obtained after mechanical grinding of SHS products. The particle size of the ZrB_2 powder was 4.58 ± 0.30 μm, and that of TaB_2 was 1.02 ± 0.11 μm. Apparently, TaB_2 is a more brittle material and, therefore, its mechanical grinding was more significant, which led to the formation of a fine-grained structure during subsequent sintering. The grain size distribution of TaB_2 is in a narrower range in the case of sintering of the SHS product. The formation of regions with small grains (less than 10 μm) in reactive SPS was attributed by the authors to the presence of oxide and other impurities in the initial powders. During reactive sintering in a die, such impurities can cause the formation of structural inhomogeneities. In this case, the combination of SHS and SPS techniques contributes to the formation

of a more uniform microstructure than in reactive sintering, which also has a positive effect on the strength properties of ceramic. The presence of pores distributed mainly in grains is associated with the presence of impurities in the initial powders, which evaporate at high temperatures during sintering.

At room temperature, the mechanical strength of ZrB_2 obtained by sintering SHS products is at the same level (≈400 MPa) as that of ZrB_2 synthesized by reactive SPS [34]. For ZrB_2 ceramic obtained by sintering of SHS products, the ultimate strength at a temperature of 1200°C is only 7% lower than the ultimate strength of ZrB_2 synthesized in reactive SPS and is 380 MPa. The fracture toughness K_{Ic} of ZrB_2 ceramic obtained using these two approaches is ≈2.2 MPa · $m^{0.5}$. Thus, the combination of mechanical activation, SHS, and SPS is promising for obtaining fine-grained single-phase ZrB_2 ceramic with low residual porosity. In [26], it is noted that the mechanical properties of TaB_2 are much inferior to those of ZrB_2 despite the smaller grain size, and this is attributed to the higher porosity of TaB_2 samples.

Sani et al. [35] obtained single-phase TiB_2 ceramic by combining mechanical activation, SHS, and SPS. The SHS product in this case contained 96% TiB_2 and had cubic and orthorhombic TiB phases, which were apparently formed due to the lack of boron in the reaction mixture. Subsequent sintering resulted in the formation of a nonporous consolidated material, which also contained TiB phases. The effect of SPS conditions on the relative density of titanium diboride was investigated. The authors note that during sintering of the SHS product at a current strength of 950 A, which corresponds to a temperature of 1530°C, a holding time of 20 min at a pressure of 60 MPa, the relative density of TiB_2 was 99.45%, and with a further increase in the current strength to 1000 A ($T \approx 1575$°C), a nonporous material was obtained. During sintering of the SHS product at a current of 950 A, the density of the sample exceeds 95% at a holding time of 5 min and approaches 100% at 20 min. The grain size of the material was less than 15 μm.

As noted above, it follows from a number of studies that for sintering of SHS products, milder conditions are needed than for obtaining the product by reactive sintering. At the same time, in [36], TiB_2 with a submicron grain size and a relative density over 99% was obtained in reactive SPS at a very low temperature of 800°C. To obtain a powder mixture that could be sintered under the specified conditions, long preliminary mechanical activation of the mixture of the reactants (for 8 h) was required. Compared with this synthesis technique, obtaining ceramic by combining SHS and SPS requires much less time. Ceramic with a relative density of 97% was produced by SPS of a commercially available TiB_2 powder with a medium grain size of 1–2 μm at a temperature of 1800°C and a pressure of 50 MPa [37]. Under heating to 1500°C the density of the material reached only 78%. Comparison of the results of these studies leads to the conclusion that powders obtained by SHS have a better capability for deformation and consolidation during SPS, apparently due to the high density of structural defects.

Using traditional sintering of TiB_2 powders without pressure, Khanra and Godkhindi [38] were able to consolidate the SHS product to a relative density of 97% and the commercially available powder only to 85.5%, which, in the opinion of these authors, is due to the difference in the density of crystal structure defects in these powders. A number of papers reported on defects in the crystal structure of SHS products. The high dislocation density in SHS products was confirmed experimentally for ZrB_2 [39]. In the SHS product, the dislocation density was 10^{12} cm^{-2}, and in ZrB_2 obtained by carbothermal reaction, it was 10^8 cm^{-2}. The influence of the method of preparing the powder to be sintered on the density of the consolidated material for SPS was also found in the synthesis of nickel boride Ni_3B [40]. The material obtained by reactive SPS had a higher relative density (≈93%) than the material obtained by SPS of the thermal explosion product (≈89%). The mass content of the Ni_2B impurity phase was 4% in the case of sintering of the product of thermal explosion and 1% in the case of reactive sintering. The grain size of the sintered materials was 1–2 μm (Fig. 3).

Moskovskikh et al. [41] obtained silicon carbide (SiC) with low residual porosity by combining mechanical activation, SHS, and SPS. The time of high-energy mechanical treatment of initial silicon powders and lamp soot was varied from 5 to 180 min. The product of mechanical treatment consisted of amorphous carbon agglomerates in which silicon nanoparticles were distributed—this structure makes it possible to reduce the synthesis temperature [41]. The theoretical density of silicon carbide is 3.21 g/cm^3. Silicon carbide obtained in this work by the SHS–SPS techniques had a density of 3.1 g/cm^3 and was sintered at a pressure of 50 MPa, a temperature of 2000°C and a holding time of 10 min. Pressure was applied to the powder at room temperature and remained constant throughout the SPS process. The SiC sample obtained by reactive sintering under the same conditions had a higher residual porosity—its density was 2.8 g/cm^3. It is noted that during reactive SPS under the same mechanical pressure throughout the sintering process, failure of punches and equipment very often occurs. In the case of reactive sin-

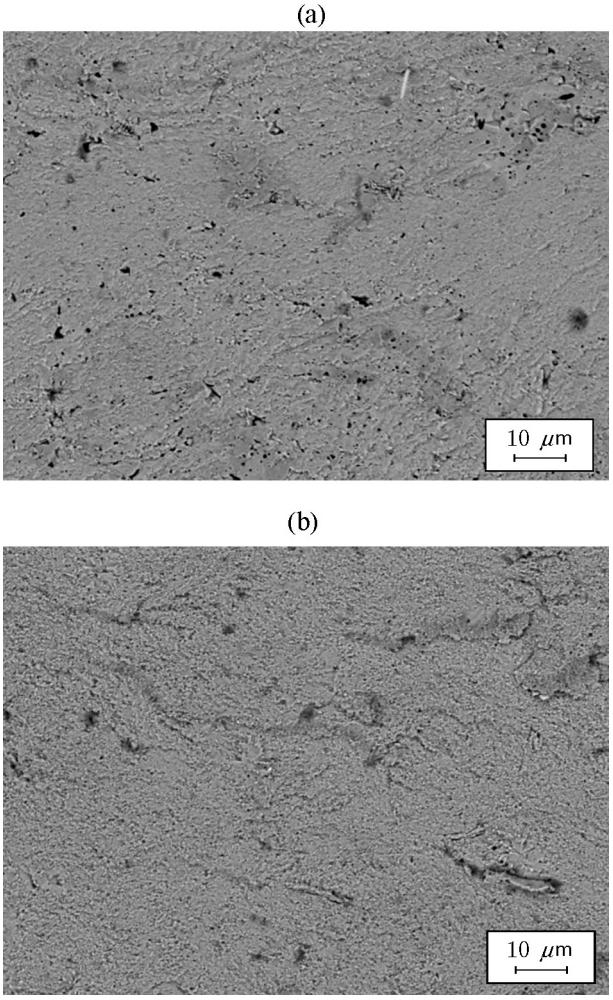

Fig. 3. Micrographs of fracture surfaces of compacts obtained by SPS of the thermal explosion product of a 3Ni–B mixture (a) and by reactive SPS of this mixture (b) [40].

tering, the most effective approach is the one where the pressure applied to the powder sample is increased after the start of synthesis and heating is started at low applied pressure. A two-stage procedure of applying pressure was also described in [24–26]. The grain sizes of SiC obtained by reactive and nonreactive methods differ [41]. In the case of sintering of the SHS product, the grain size of the ceramic was 200–300 nm, and in reactive sintering, the grain size of the product was >3 μm. In both cases, the sintered samples demonstrated intergranular fracture. The same differences in grain size were observed in a comparative study of the synthesis of ZrB_2 and TaB_2 [26]. According to [41], the difference in grain size is due to the additional heat release from the exothermic reaction during reactive sintering, which contributes to additional crystallite growth. Despite the difference in grain sizes, silicon carbide ceramic samples had close microhardness values (24 ± 1 GPa) [41]. However, their fracture toughness values were different: 4 MPa $\cdot$ m$^{0.5}$ for the sample obtained by sintering the SHS product, and 5 MPa $\cdot$ m$^{0.5}$ for the product of reactive SPS. Probably, the lowered fracture toughness of SiC obtained by SHS–SPS is due to the greater imperfection of the structure typical of SHS products and preserved during sintering.

Examples of the preparation of metal silicides by SHS and SPS techniques are also described in the literature. Shimizu et al. [42] obtained molybdenum disilicide $MoSi_2$ by SPS (1300°C, 10 min, and 30 MPa) of SHS products. In the structure of ceramic, there were pores distributed mainly along the grain boundaries. The average grain size was 7.5 μm. The authors note that, in addition to $MoSi_2$, the SHS product also contained the Mo_5Si_3 phase, which was preserved after SPS. It should be noted that the reactants were not subjected to preliminary mechanical treatment before SHS. Cabouro et al. [43] obtained $MoSi_2$ ceramic by reactive SPS of a mechanically activated mixture of molybdenum and silicon at temperatures of 1573–1773 K. The authors note that the synthesis of $MoSi_2$ requires melting of silicon (T_{melt} = 1688 K). Increasing the sintering temperature led to an increase in the crystallite size of $MoSi_2$ and to a decrease in the hardness and fracture toughness of the material. Generally, the mechanical properties of $MoSi_2$ ceramic obtained by SHS–SPS [42] and reactive SPS [43] can vary depending on the synthesis conditions and are comparable to each other.

Kurbatkina et al. [44, 45] obtained (Ta, Hf)C and (Ta, Zr)C ternary carbides by SPS of SHS products. In the case of (Ta, Hf)C, mechanical activation of the starting reactants reduced the combustion temperature by more than 800°C compared to the adiabatic temperature (3001°C). The high rate of the SHS process hinders in the formation of complex (ternary) carbides from metal powders and carbon black. Quite often, the synthesis products contain, in addition to ternary carbides, and MeC carbides. These authors obtained single-phase (Ta, Hf)C ternary carbide by combustion of a mechanically activated mixture of Ta + C + HfC. In addition to the main phase, the SHS products contained (less than 3%) HfO_2 and ZrO_2 oxide impurities. Dissolution of oxygen in metals occurred during mechanical treatment of the powders without the use of a protective medium (in air). The synthesis products were mechanically ground to a size of 1–3 μm and sintered at different temperatures. The relative density of (Ta Hf)C obtained by plasma spark sintering (2000°C, 10 min, and 50 MPa) was 93%, and the density of (Ta, Zr)C was ≈99%. (Ta, Hf)C and (Ta, Zr)C

ternary carbides contained micro- and nanosized pores, which were distributed both along the boundaries and within the grains. During SPS of ternary carbides, the grain size increased on average from 1–3 to 10–15 μm. The Young's modulus of carbides was estimated (using a nanohardness tester) from loading and unloading curves. Values of 423.6 ± 45 GPa were obtained for (Ta, Hf)C, and 536.47 ± 28.7 GPa for (Ta, Zr)C.

The synthesis of high-entropy compounds is currently one of the most important problems of materials science. The possibility of obtaining high-entropy diborides by SPS of SHS products was shown by Tallarita et al. [46]. Single-phase diboride $(Hf_{0.2}Mo_{0.2}Ta_{0.2}Nb_{0.2}Ti_{0.2})B_2$ with a relative density of 92.5% (SPS, 20 min, 20 MPa, and 1950°C) was obtained. In [47, 48], consolidated high-entropy borides and carbides were obtained by reactive SPS of mechanically treated mixtures of reactants. The time of preliminary mechanical treatment of reaction mixtures was 6–24 h. The synthesis technique proposed in [46], which involves mechanical activation of a mixture of initial powders for 20 min with subsequent SHS, allows a significant reduction in the time of the entire process. The SHS product contained about 4% of impurity phases [$(Ta_{0.5}Ti_{0.5})B_2$, $(Hf_{0.5}Ti_{0.5})B_2$, HfB_2, and HfO_2]; subsequent SPS resulted in ultra-high-temperature diboride $(Hf_{0.2}Mo_{0.2}Ta_{0.2}Nb_{0.2}Ti_{0.2})B_2$.

SYNTHESIS OF CERAMIC COMPOSITES

Ceramic matrix composites have higher fracture toughness than single-phase ceramics. To obtain ceramic composites by SHS, various methods of product consolidation are used. In [49–51], ZrB_2–CrB and WC–W_2C composites were obtained using electric thermal explosion, which is an SHS process carried out under pressure and initiated by electric current. In [52, 53], $TaSi_2$–SiC and $MoSi_2$–HfB_2–MoB composites were obtained by hot pressing of SHS products. In [54], a composite powder of ZrB_2–ZrC was first synthesized by SHS in a mechanically activated Zr–B–C mixture, and then a composite with a relative density of 98% was obtained by SPS (5 min, 40 MPa, and 1800°C). A comparison of this composite with the composite produced by SPS of a mixture of commercially available ZrB_2 and ZrC powders was performed. Sintering of SHS products led to the formation of a more uniform structure with an average grain size of 5 μm, which corresponds to the size of agglomerates after mechanical grinding of combustion products. The preservation of grain sizes indicates the suppression of recrystallization processes during SPS at a short holding time. The relative density of the composite from the commercial powders was significantly lower (89%). The microhardness of the composite formed by SHS–SPS was 17.8 GPa, and the fracture toughness was 3.8 $MPa \cdot m^{0.5}$. The microhardness of the composite formed during sintering of commercial powders was 16.6 GPa, and its fracture toughness was 3.4 $MPa \cdot m^{0.5}$. Comparison made in that work shows that combining mechanical activation, SHS, and SPS makes it possible to obtain ceramic matrix composites with low porosity and mechanical properties that are not inferior to those of ceramics obtained by conventional methods.

Obtaining composites with low residual porosity is a difficult task in the case where the starting reactants are refractory metals. NbC/NbB_2 composites were obtained by Tsuchida and Kakuta [55]. A feature of their work is that mechanical treatment of a mixture of Nb/B/C = 2/2/1 in air for 105 min led to their self-ignition, resulting in the formation of NbC and NbC/NbB_2 phases. After mechanical treatment, the niobium phase was also present, indicating that the synthesis reactions were not completed. After SPS (1800°C, 10 min, and 40 MPa), the relative density of the composite was 91%, and it contained Nb_3B_4 and graphite. The sample obtained by reactive SPS of a powder mixture Nb/B/C = 2/2/1 not subjected to preliminary mechanical treatment had a higher relative density (96.7%). The formation of a large number of pores during sintering of SHS products was attributed by the authors to the presence of unreacted carbon and boron. To obtain a composite with a lower porosity, residual carbon and boron were removed from the SHS products by dissolving them in tetrabromoethane. After SPS, this material contained the Nb_3B_4 phase, but the porosity was significantly reduced (relative density was increased to 94%). The resulting material had a higher hardness (19.8 GPa) than the materials produced by sintering the SHS product (13.3 GPa) and reactive sintering (14.3 GPa).

Musa et al. [56] performed the synthesis of $TiC_{0.7}/TiB_2$ powders with their subsequent SPS. It is interesting that to obtain a nanostructured composite powder, the authors used quenching, i.e., rapid cooling of the SHS products (in water). In this work, the reactants were Ti, B_4C, and graphite. The agglomerates formed in this way consisted of nanosized grains of $TiC_{0.7}$ and TiB_2 uniformly distributed over the volume of particles. Optimal SPS conditions (1400°C, 3 min, and 20 MPa) for obtaining a consolidated material with a relative density >99.9 % were determined. Mixing in the range 60–90 s is associated with a redistribution of powder particles and their compaction. Fast mix-

ing after 120 s is associated with sintering processes. The main compaction of the sample after sintering took place in the temperature range 800–1200°C. The authors note that in other studies (using hot pressing [57] or SPS of commercial powders [58]) much higher pressure and higher holding temperature were required to obtain dense ceramics of the same composition.

Kasraeeet al. [59] obtained Ti_5Si_3–TiC composite by SPS of SHS combustion products of a mechanically activated Ti–Si–C mixture. A uniform distribution of the phases of the composite can be achieved by mechanical activation before synthesis. Activation leads to the formation of a large number of crystal structure defects, which subsequently act as centers of nucleation and growth of new phases. Moreover, diffusion distances decrease due to a more uniform distribution of reactants in the mixture and grain-size reduction. Mechanical activation also decreases the combustion temperature. In [59], a powder product of the composition Ti_5Si_3 + TiC was obtained by SHS after mechanical treatment of reactants for 2 h. In the SPS of the SHS product, the formation of a nonporous material occurred at 450°C (at 50 MPa), which is a fairly low temperature. As noted above, this high sinterability is explained by the high defect concentration in SHS powders. In turn, grain size reduction improves the mechanical properties of ceramic materials. After sintering, the sample was annealed to relieve internal stresses. Due to the uniform distribution of fine TiC grains in the Ti_5Si_3 matrix, the fracture toughness was 4.7 ± 0.1 MPa $\cdot$ m$^{0.5}$, which is higher than that of single-phase Ti_5Si_3 [60] and Ti_5Si_3–TiC composites obtained by other methods.

Combining SHS and SPS techniques makes it possible to obtain ceramics consisting of three phases. HfB_2–HfC–SiC composite was obtained in this way in [61]. The synthesis was carried out by the reaction

$$8Hf + 2B_4C + 1.5Si + 3.5C \rightarrow 4HfB_2 + 4HfC + 1.5SiC.$$

A composite consisting entirely of the required phases was obtained by SHS of a mixture of reactants mechanically activated for 20 min. SPS of the composite powder (1800°C, 20 MPa, 30 min) resulted in a material with a relative density over 98.5%. Slight grain growth was observed during sintering. The phases were evenly distributed in the volume of the sample. The fracture toughness of the HfB_2–HfC–SiC composite was 6.2 ± 0.7 MPa $\cdot$ m$^{0.5}$, which is high for ceramic materials.

SYNTHESIS OF INTERMETALLICS

The SPS technique can be used to synthesize and consolidate various intermetallic compounds. Shevtsova et al. [62] obtained Ni_3Al intermetallic compound by reactive SPS at a temperature of 1100°C, a pressure of 40 MPa, and a holding time of 5 min. Preliminary mechanical treatment of initial nickel and aluminum powders made it possible to reduce the porosity of the sintered material and to obtain more uniform microstructure. Samples sintered from an unactivated mixture of powders contained the NiAl phase. This difference in structure is due to additional mixing of components and a reduction in diffusion distances during mechanical treatment.

FeAl intermetallic compound was synthesized by Paris et al. [63] using reactive SPS. After mechanical treatment of a mixture of iron and aluminum for 4 h, a nanostructured powder was obtained. Reactive SPS was chosen as it is a one-step process. Comparative study of SHS–SPS and reactive SPS was not carried out. Due to the fact that during SPS, the sample is held at a high temperature for a short time, the use of this technique made it possible to preserve the nanostructured state of the material after sintering. The crystallite size of the sintered FeAl intermetallic compound calculated from the X-ray diffraction pattern was different for different directions: 30 nm for the (h00) direction and 50 nm for the (hh0) direction. The authors attribute the difference in crystallite sizes to the deformation of the material under mechanical pressure during SPS. The crystallite size of the FeAl intermetallic compound obtained by SHS was ≈35 nm and did not depend on the direction of the crystal lattice.

It has been shown [64] that in the case of the formation of a composite with a FeAl matrix reinforced with Y_2O_3 yttrium oxide, SPS allows obtaining a material in which the reinforcing particles are evenly distributed throughout the volume. In this work, a mechanically treated mixture of FeAl and Y_2O_3 powders was sintered at a pressure of 70 MPa. The obtained material contains micron-size grains. It was found that at high sintering temperatures, the oxide shells of the particles were destroyed, and at low temperatures, this effect was not observed. The authors note that SPS is a complex process in which the formation of the material structure is determined by several physical mechanisms such as plastic flow and melt formation.

Paris et al. [65] synthesized FeAl intermetallic compound by combustion of a mechanically activated mixture of iron and aluminum. The reaction was carried out under the simultaneous action of pressure and an electric current. The synthesis time was 3–5 min, and the maximum temperature during combustion reached 1300°C. The obtained samples were annealed in the chamber of an experimental setup, where X-ray diffraction patterns of the sample were recorded during heating. A significant grain growth during annealing in the

temperature range 450–800°C was observed. Increasing the annealing temperature reduced the hardness of the intermetallic compound, which is associated with the growth of grains of the material.

SYNTHESIS OF METAL MATRIX COMPOSITES

Today, there are many methods for obtaining metal matrix composites. The possibility of obtaining such composite materials by SHS is demonstrated in [66, 67]. Features of the synthesis of composite powders with a titanium binder and the processes occurring during their sintering are discussed in [68]. Combining SHS and SPS techniques allows obtaining metal matrix composites with improved mechanical properties compared to composites obtained by traditional methods. Ti–TiC composites were obtained in this way by Lagos et al. [69]. The starting reactants were Ti–6Al–4V alloy powder and carbon black. In the first stage, TiC was synthesized by SHS with the addition of excess titanium to the reaction mixture. The chosen approach provides the formation of a structure in which TiC particles are surrounded by titanium. During high-temperature synthesis, titanium is in a molten state and coats the resulting TiC particles, thus providing good adhesion at the interface. Before SPS, the required amount of Ti–6Al–4V powder was added to the SHS product for the formation of Ti–5%(vol.) TiC and Ti–10%(vol.) TiC composites. Sintering of metal matrix composites requires lower temperature than in the case of sintering of ceramic composites. Sintering of composites with a titanium alloy matrix was carried out at a temperature of 1100°C and a pressure of 20 MPa for 2 min. The composite matrix has lamellar structure, and the size of TiC particles does not exceed 30 μm.

The possibility of obtaining large disk-shaped samples of this composite with a diameter of 200 mm was also shown in [69]. Significant differences in the microstructure of the sample in its different regions were not found. The ultimate strength of this composite is higher than that of the matrix alloy obtained by SPS.

The synthesis of copper matrix composites by combining SHS and SPS is described in [70]. During grinding and mechanical treatment of 57%(vol.) TiB_2–Cu composite powder (SHS products), additional copper was added to it to obtain 4.5%(vol.) TiB_2–Cu composites. SHS of powders with a high copper content is not possible due to difficulties in combustion. In the first case (method 1), the copper powder was added in the required amount immediately before treatment in a mill. In the second case (method 2), the SHS product was preliminarily treated in a mill, and then copper powder was added to it. The authors note that mechanical treatment of the mixture of reactants (Ti–B–Cu) before SHS is needed to obtain submicron TiB_2 particles in the copper matrix and to reduce the combustion temperature. During SPS of agglomerates of 4.5%(vol.) TiB_2–Cu (50 MPa and 650°C), composites were obtained in which TiB_2 particles are uniformly distributed in the volume of the matrix. The relative density of the composites obtained by method 1 was somewhat lower (96–98%) than when using method 2 (>98%). Due to the more efficient grinding of the SHS product in method 2, the material produced by this method had a more uniform structure than that produced by method 1. Using method 2, higher material hardness was achieved. The microstructure of the material is shown in Fig. 4.

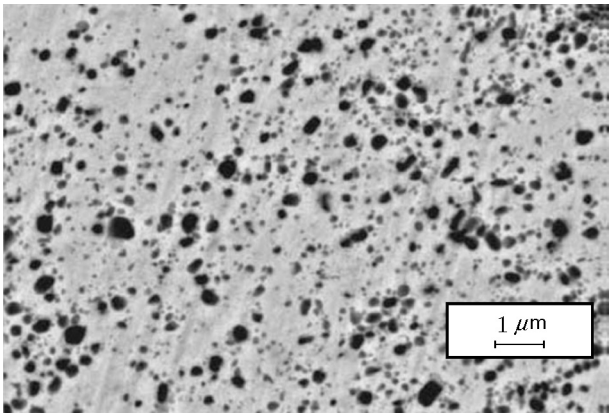

Fig. 4. Microstructure of 4.5%(vol.) TiB_2–Cu composite obtained by SPS at 650°C (SHS product was mechanically treated with an additional amount of a copper powder [70]).

The authors of the present review obtained TiC–Cu composites using reactive SPS [71]. Titanium carbide particles were synthesized by the reaction between $Ti_{25}Cu_{75}$ alloy and carbon (carbon black or nanodiamonds) in a mechanically activated mixture of powders. It has been found that the reaction diffusion of titanium in the alloy to the interfaces between alloy particles and carbon plays an important role in structure formation processes.

CONCLUSIONS

The approach considered in this review, consisting in SPS of SHS products, allows obtaining single-phase ceramic materials, ceramic and metal matrix composites, and intermetallics. The relative density of such

materials can be 90–100% with a proper choice of sintering conditions. SPS of SHS products leads to the formation of a finer-grained structure compared with reactive sintering. It is suggested that grain growth during reactive SPS is associated with additional heat release during exothermic reactions. At the same time, the characteristic features of SHS products, such as a small grain size and internal stresses, are preserved at a short holding time of SPS.

The features of the structure of materials produced by SPS of SHS products include the presence of oxide and other impurities that can lead to the formation of closed pores during sintering.

It should be noted that sintering of SHS products is a more advanced and productive technique for obtaining single-phase and composite ceramic materials than reactive sintering. In order for the synthesis in reactive SPS to be complete, mechanical activation of the mixture of reactants for a long time (from a few hours to one day) is often required. Mechanical treatment of powders leads to additional mixing of components, an increase in the defect concentration in the structure, and a decrease in diffusion distances. In the case of sequential use of SHS–SPS, the time of mechanical treatment of the starting reactants can be reduced to 5–20 min. The duration of subsequent SHS also takes a few minutes on average.

The high sinterability of SHS products due to the high defect concentration in their structure is noted in many papers. Accordingly, sintering of SHS products makes it becomes possible to reduce the sintering temperature and the holding time.

In the case of metal matrix composites, obtaining SHS products with a high content of metal binder (not involved in the exothermic reaction) seems impossible to due to difficulties in the synthesis in such reaction mixtures. Adding the required amount of metal powders after mechanical grinding of the SHS product solves this problem and allows the formation of composites of the required composition in subsequent SPS. The SPS and SHS techniques can also be employed to synthesize nanostructured intermetallic compounds and use them to obtain compacts with low residual porosity.

Materials with low residual porosity and fine-grained structure obtained by SPS of SHS products have promising mechanical properties (high fracture toughness, Young's modulus, hardness, and strength).

REFERENCES

1. A. S. Rogachev and A. S. Mukas'yan, *Combustion for the Synthesis of Materials* (Fizmatlit, Moscow, 2012) [in Russian].
2. A. G. Merzhanov, "Self-Propagating High-Temperature Synthesis," in *Physical chemistry. Contemporary Problems*, Ed. by Ya. M. Kolotyrkin (Khimiya, Moscow, 1983), pp. 6–45 [in Russian].
3. A. S. Rogachev, A. S. Mukas'yan, and A. G. Merzhanov, "Structure Transformation in Gasless Combustion of Titanium–Carbon and Titanium–Boron Systems," Dokl. Akad. Nauk SSSR **297** (6), 1425–1428 (1987).
4. A. G. Merzhanov, "History and Recent Developments in SHS," Ceram. Int. **21** (5), 371–379 (1995).
5. P. Mossino, "Some Aspects in Self-Propagating High-Temperature Synthesis," Ceram. Int. **30** (3), 311–332 (2004).
6. E. Pocheć, S. Jóźwiak, K. Karczewski, and Z. Bojar, "Fe–Al Phase Formation around SHS Reactions under Isothermal Conditions," J. Alloys Compd. **509** (4), 1124–1128 (2011).
7. V. E. Ovcharenko, O. V. Lapshin, E. N. Boyangin, I. S. Ramazanov, and V. A. Chudinov, "High-Temperature Synthesis of Ni_3Al Intermetallic Compound under Pressure," Izv. Vyssh. Uchebn. Zaved. Tsv. Metallurg., No. 4, 63–69 (2007).
8. G. Tosuna, L. Ozlerb, M. Kayac, and N. Orhand, "A Study on Microstructure and Porosity of NiTi Alloy Implants Produced by SHS," J. Alloys Compd. **487** (1/2), 605–611 (2009).
9. O. P. Solonenko, V. E. Ovcharenko, V. Yu. Ulianitsky, A. E. Chesnokov, I. S. Batraev, "Effect of the Microstructure of SHS Powders of Titanium Carbide-Nichrome on the Properties of Detonation Coatings," J. Surf. Invest.: X-ray, Synchr. Neutr. Tech. **10** (5), 1040–1047 (2016).
10. O. K. Lepakova, L. G. Raskolenko, and Y. M. Maksimov, "Self-Propagating High-Temperature Synthesis of Composite Material TiB_2–Fe," J. Mater. Sci. **39** (11), 3723–3732 (2004).
11. M. S. Song, M. X. Zhang, S. G. Zhang, B. Huang, and J. G. Li, "In situ Fabrication of TiC Particulates Locally Reinforced Aluminum Matrix Composites by Self-Propagating Reaction during Casting," Mater. Sci. Eng. A **473** (1/2), 166–171 (2008).
12. Y.-S. Kwon, D. V. Dudina, M. A. Korchagin, O. I. Lomovsky, and H.-S. Kim, "Solid State Synthesis of Titanium Diboride in Copper Matrix," J. Metastab. Nanocryst. Mater. **15/16**, 253–258 (2003).
13. E. A. Olevsky and D. V. Dudina, *Field-Assisted Sintering: Science and Applications* (Springer, Cham, 2018).
14. R. Orrù, R. Licheri, A. M. Locci, A. Cincotti, and G. Cao, "Consolidation/Synthesis of Materials by Electric Current Activated/Assisted Sintering," Mater. Sci. Eng. R **63** (4-6), 127–287 (2009).

15. Z. A. Munir andU. Anselmi-Tamburini, "The Effect of Electric Field and Pressure on the Synthesis and Consolidation of Materials: A Review of the Spark Plasma Sintering Method," J. Mater. Sci. **41** (3), 763–777 (2006).
16. E. A. Olevsky, "Impact of Thermal Diffusion on Densification during SPS," J. Am. Ceram. Soc. **92** (S1), S122–S132 (2009).
17. T. B. Holland, T. B. Tran, D. V. Quach, U. Anselmi-Tamburini, J. R. Groza, and A. K. Mukherjee, "Athermal and Thermal Mechanisms of Sintering at High Heating Rates in the Presence and Absence of an Externally Applied Field," J. Eur. Ceram. Soc. **32** (14), 3675–3683 (2012).
18. Z.-H. Zhang, Z.-F. Liu, J.-F. Lu, X.-B. Shen, F.-C. Wang, and Y.-D. Wang, "The Sintering Mechanism in Spark Plasma Sintering—Proof of the Occurrence of Spark Discharge," Scripta Mater., No. 81, 56–59 (2014).
19. D. M. Hulbert, A. Anders, D. V. Dudina, J. Andersson, D. Jiang, C. Unuvar, U. Anselmi-Tamburini, E. J. Lavernia, and A. K. Mukherjee, "The Absence of Plasma in 'Spark Plasma Sintering'," J. Appl. Phys. **104** (3), Article number 033305 (2008).
20. V. Mamedov, "Spark Plasma Sintering As Advanced PM Sintering Method," Powder Metall. **45** (4), 322–328 (2002).
21. R. Orrù andG. Cao, "Comparison of Reactive and Non-Reactive Spark Plasma Sintering Routes for the Fabrication of Monolithic and Composite Ultra High Temperature Ceramics (UHTC) Materials," Materials **6** (5), 1566–1583 (2013).
22. C. Musa, R. Orrù, D. Sciti, L. Silvestroni, andG. Cao, "Synthesis, Consolidation and Characterization of Monolithic and SiC Whiskers Reinforced HfB_2 Ceramics," J. Eur. Ceram. Soc. **33**, (3), 603–614 (2013).
23. C. Musa., R. Orrù, D. Sciti, and G. Cao, "Spark Plasma Synthesis and Densification of TaB_2 by Pulsed Electric Current Sintering," Mater. Lett. **65** (19/20), 3080–3082 (2011).
24. R. Licheri, R. Orrù, A. M. Locci, and G. Cao, "Efficient Synthesis/Sintering Routes to Obtain Fully Dense ZrB_2–SiC Ultra-High-Temperature Ceramics (UHTCs)," Ind. Eng. Chem. Res. **46** (26), 9087–9096 (2007).
25. R. Licheri, R. Orrù, C. Musa, and G. Cao, "Synthesis, Densification and Characterization of TaB_2–SiC Composites," Ceram. Int. **36** (3), 937–941 (2010).
26. R. Licheri, C. Musa, R. Orrù, G. Cao, D. Sciti, and L. Silvestroni, "Bulk Monolithic Zirconium and Tantalum Diborides by Reactive and Non-Reactive Spark Plasma Sintering," J. Alloys Compd., No. 663, 351–359 (2016).
27. M. A. Korchagin, T. F. Grigor'iev, B. B. Bokhonov, M. R. Sharafutdinov, A. P. Barinova, and N. Z. Lyakhov, "Solid-State Combustion in Mechanically Activated SHS Systems. I. Effect of Activation Time on Process Parameters and Combustion Product Composition," Fiz. Goreniya Vzryva **39** (1), 51–59 (2003) [Combust., Expl., Shock Waves **39** (1), 43–50 (2003); https://doi.org/10.1023/A:1022145201911].
28. M. A. Korchagin and D. V. Dudina, "Application of Self-Propagating High-Temperature Synthesis and Mechanical Activation for Obtaining Nanocomposites," Fiz. Goreniya Vzryva **43** (2), 58–71 (2007) [Combust., Expl., Shock Waves **43** (2), 176–187 (2007); https://doi.org/10.1007/s10573-007-0024-3].
29. M. A. Korchagin, E. G. Avvakumov, G. G. Lepezin, and O. B. Vinokurova, "Thermal Explosion and Self-Propagating High-Temperature Synthesis in Mechanically Activated SiO_2–Al Mixtures," Fiz. Goreniya Vzryva **50** (6), 21–27 (2014) [Combust., Expl., Shock Waves **50** (6), 641–646 (2014); https://doi.org/10.1134/S0010508214060033].
30. M. A. Korchagin, "Thermal Explosion in Mechanically Activated Low-Calorific-Value Compositions," Fiz. Goreniya Vzryva **51** (5), 77–86 (2015) [Combust., Expl., Shock Waves **51** (5), 578–586 (2015); https://doi.org/10.1134/S0010508215050093].
31. M. A. Korchagin, A. I. Gavrilov, B. B. Bokhonov, N. V. Bulina, and V. E. Zarko, "Synthesis of Aluminum Diboride by Thermal Explosion in Mechanically Activated Mixtures of Initial Reactants," Fiz. Goreniya Vzryva **54** (4), 45–54 (2018) [Combust., Expl., Shock Waves **54** (4), 424–432 (2018); https://doi.org/10.1134/S0010508218040068].
32. M. A. Korchagin and N. V. Bulina, "Superadiabatic Regime of Thermal Explosion in a Mechanically Activated Mixture of Tungsten with Carbon Black," Fiz. Goreniya Vzryva **52** (2), 112–121 (2016)[Combust., Expl., Shock Waves **52** (2), 225–233 (2016); https://doi.org/10.1134/S0010508216020131].
33. R. Licheri, C. Musa, R. Orrù, and G. Cao, "Influence of the Heating Rate on the in-situ Synthesis and Consolidation of ZrB_2 by Reactive Spark Plasma Sintering," J. Eur. Ceram. Soc. **35** (4), 1129–1137 (2015).
34. E. Zapata-Solvas, D. D. Jayaseelan, H. T. Lin, P. Brown, and W. E. Lee, "Mechanical Properties of ZrB_2- and HfB_2-Based Ultra-High Temperature Ceramics Fabricated by Spark Plasma Sintering," J. Eur. Ceram. Soc. **33** (4), 1373–1386 (2013).
35. E. Sani, M. Meucci, L. Mercatelli, A. Balbo, C. Musa, R. Licheri, R. Orrù, and G. Cao, "Titanium Diboride Ceramics for Solar Thermal Absorbers," Sol. Energy Mater. Sol. Cells **169**, 313–319 (2017).

36. N. S. Karthiselva, B. S. Murty, and S. R. Bakshi, "Low Temperature Synthesis of Dense TiB_2 Compacts by Reaction Spark Plasma Sintering," Int. J. Refract. Met. Hard Mater. **48**, 201–210 (2015).
37. Z. H. Zhang, X. B. Shen, F. C. Wang, S. K. Lee, and L. Wang, "Densification Behavior and Mechanical Properties of the Spark Plasma Sintered Monolithic TiB_2 Ceramics," Mater. Sci. Eng. A **527** (21/22), 5947–5951 (2010).
38. A. K. Khanra andM. M. Godkhindi, "Comparative Studies on Sintering Behavior of Self-Propagating High-Temperature Synthesized Ultra-Fine Titanium Diboride Powder," J. Am. Ceram. Soc. **88** (6), 1619–1621 (2005).
39. S. K. Mishra, S. Das, and L. C. Pathak, "Defect Structures in SHS Produced Zirconium Diboride Powders," Mater. Sci. Eng. A **64** (1/2), 249–255 (2004).
40. A. V. Ukhina, D. V. Dudina, M. A. Korchagin, Yu. G. Mateishina, N. V. Bulina, A. G. Anisimov, V. I. Mali, and I. S. Batraev, "Synthesis and Compaction of Nickel Boride Ni_3B by Spark Plasma Sintering," Khim. Interes. Ustoich. Razv. **24** (2), 203–208 (2016).
41. D. O. Moskovskikh, Y. Song, S. Rouvimov, A. S. Rogachev, A. S. Mukasyan, "Silicon Carbide Ceramics: Mechanical Activation, Combustion and Spark Plasma Sintering," Ceram. Int. **42** (11), 12686–12693 (2016).
42. H. Shimizu, M. Yoshinaka, K. Hirota, and O. Yamaguchi, "Fabrication and Mechanical Properties of Monolithic $MoSi_2$ by Spark Plasma Sintering," Mater. Res. Bull. **37** (9), 1557–1563 (2002).
43. G. Cabouro, S. Chevalier, E. Gaffet, Grin Yu, and F. Bernard, "Reactive Sintering of Molybdenum Disilicide by Spark Plasma Sintering from Mechanically Activated Powder Mixtures: Processing Parameters and Properties," J. Alloys Compd. **465** (1/2), 344–355 (2008).
44. V. V. Kurbatkina, E. I. Patsera, E. A. Levashova, and A. N. Timofeev, "Self-Propagating High-Temperature Synthesis of Single-Phase Binary Tantalum–Hafnium Carbide (Ta, Hf)C and Its Consolidation by Hot Pressing and Spark Plasma Sintering," Ceram. Int. **44** (4), 4320–4329 (2018).
45. V. V. Kurbatkina, E. I. Patsera, S. A. Vorotilo, E. A. Levashov, and A. N. Timofeev, "Conditions for Fabricating Single-Phase (Ta, Zr)C Carbide by SHS from Mechanically Activated Reaction Mixtures," Ceram. Int. **42** (15), 16491–16498 (2016).
46. G. Tallarita, R. Licheri, S. Garroni, R. Orrù, and G. Cao, "Novel Processing Route for the Fabrication of Bulk High-Entropy Metal Diborides," Scripta Mater. **158**, 100–104 (2019).
47. J. Gild, Y. Zhang, T. Harrington, S. Jiang, T. Hu, M. C. Quinn, W. M. Mellor, N. Zhou, K. Vecchio, and J. Luo, "High-Entropy Metal Diborides: A New Class of High-Entropy Materials and a New Type of Ultrahigh Temperature Ceramics," Sci. Rep. **6**, Article number 37946 (2016).
48. M. Castle, T. Csanádi, S. Grasso, J. Dusza, and M. Reece, "Processing and Properties of High-Entropy Ultra-High Temperature Carbides," Sci. Rep. **8**, Article number 8609 (2018).
49. A. V. Shcherbakov, V. A. Shcherbakov, V. Yu. Barinov, S. G. Vadchenko, and A. V. Linde, "Influence of the Mechanical Activation of Reaction Mixture on the Formation of Microstructure of ZrB_2–CrB Composites Obtained by Electrothermal Explosions under Pressure," Refract. Ind. Ceram. **60** (2), 61–64 (2019).
50. A. V. Shcherbakov, V. A. Shcherbakov, and V. Yu. Barinov, "Preparation of the ZrB_2–CrB Composites by Pressure-Assisted Electrothermal Explosion," Lett. Mater. **9** (1), 39–44 (2019).
51. V. T. Telepa, M. I. Alymov, V. A. Shcherbakov, A. V. Shcherbakov, and V. I. Vershinnikov, "Synthesis of the WC–W_2C Composite by Electro-Thermal Explosion under Pressure," Lett. Mater. **8** (2), 119–122 (2018).
52. S. Vorotilo, E. A. Levashov, V. V. Kurbatkina, D. Yu. Kovalev, and N. A. Kochetov, "Self-Propagating High-Temperature Synthesis of Nanocomposite Ceramics $TaSi_2$–SiC with Hierarchical Structure and Superior Properties," J. Eur. Ceram. Soc. **38** (2), 433–443 (2018).
53. A. Yu. Potanin, S. Vorotilo, Yu. S. Pogozhev, S. I. Rupasov, T. A. Lobova, and E. A. Levashov, "Influence of Mechanical Activation of Reactive Mixtures on the Microstructure and Properties of SHS-Ceramics $MoSi_2$–HfB_2–MoB," Ceram. Int. **45** (16), 20354–20361 (2019).
54. T. Tsuchida and S. Yamamoto, "MA-SHS and SPS of ZrB_2–ZrC Composites," Solid State Ionics **172** (1–4), 215–216 (2004).
55. T. Tsuchida and T. Kakuta, "Fabrication of SPS Compacts from NbC–NbB_2 Powder Mixtures Synthesized by the MA-SHS in Air Process," J. Alloys Compd. **415** (1/2), 156–161 (2006).
56. C. Musa, A. M. Locci, R. Licheri, R. Orrù, G. Cao, D. Vallauri, F. A. Deorsola, E. Tresso, J. Suffner, H. Hahn, P. Klimczyk, and L. Jaworska, "Spark Plasma Sintering of Self-Propagating High-Temperature Synthesized $TiC_{0.7}/TiB_2$ Powders and Detailed Characterization of Dense Product," Ceram. Int. **35** (7), 2587–2599 (2009).

57. J. Lis, S. Majorowski, V. Hlavacek, and J. A. Puszynski, "Combustion Synthesis and Densification of TiB_2–TiC Composite Powders," Int. J. Self-Propag. High-Temp. Synth. **4** (3), 275–285 (1995).
58. A. M. Locci, R. Orrù, G. Cao, and Z. A. Munir, "Simultaneous Spark Plasma Synthesis and Densification of TiC–TiB_2 Composites," J. Am. Ceram. Soc. **89** (3), 848–855 (2006).
59. K. Kasraee, M. Yousefpour, and S. A. Tayebifard, "Microstructure and Mechanical Properties of an Ultrafine Grained Ti_5Si_3–TiC Composite Fabricated by Spark Plasma Sintering," Adv. Powder Technol. **30** (5), 992–998 (2019).
60. K. Kasraee, M. Yousefpour, and S. A. Tayebifard, "Microstructure and Mechanical Properties of Ti_5Si_3 Fabricated by Spark Plasma Sintering," J. Alloys Compd. **779** (30), 942–949 (2019).
61. R. Licheri, R. Orrù, C. Musa, A. M. Locci, and G. Cao, "Consolidation via Spark Plasma Sintering of HfB_2/SiC and HfB_2/HfC/SiC Composite Powders Obtained by Self-Propagating High-Temperature Synthesis," J. Alloys Compd. **478** (1/2), 572–578 (2009).
62. L. I. Shevtsova, E. A. Lozhkina, V. V. Samoylenko, I. S. Ivanchik, V. I. Mali, and A. G. Anisimov, "Evaluation of Corrosion Resistance of Ni_3Al Produced by Spark Plasma Sintering of Mechanically Activated Powder Mixtures," Mater. Today: Proc. **12** (1), 116–119 (2019).
63. S. Paris, E. Gaffet, F. Bernard, and Z. A. Munir, "Spark Plasma Synthesis from Mechanically Activated Powders: A Versatile Route for Producing Dense Nanostructured Iron Aluminides," Scripta Mater. **50** (5), 691–696 (2004).
64. T. Grosdidier, G. Ji, E. Bernard, E. Gaffet, Z. A. Munir, and S. Launois, "Synthesis of Bulk FeAl Nanostructured Materials by HVOF Spray Forming and Spark Plasma Sintering," Intermetallics **14** (10/11), 1208–1213 (2006).
65. S. Paris, C. Pighini, E. Gaffet, Z. A. Munir, and F. Bernard, "Thermal Stability of FeAl Intermetallics Prepared by SHS Sintering," Int. J. Self-Propag. High-Temp. Synth. **17** (3), 183–188 (2008).
66. G. A. Pribytkov, V. V. Korzhova, A. V. Baranovskii, and M. G. Krinitsyn, "Phase Composition and Structure of SHS Composite Powders of Titanium Carbide with an R6M5 Steel Binder," Izv. Vyssh. Uchebn. Zaved. Poroshk. Metallurg. Funkts. Pokryt. **2**, 64–71 (2017).
67. G. A. Pribytkov, M. G. Krinitsyn, V. V. Korzhova, and A. V. Baranovskii, "Structure and Phase Composition of SHS Products in Powder Mixtures of Titanium, Carbon, and Aluminum," Izv. Vyssh. Uchebn. Zaved. Poroshk. Metallurg. Funkts. Pokryt **3**, 26–35 (2019).
68. A. G. Knyazeva, E. N. Korosteleva, M. G. Krinitsyn, et al., *Metal–Matrix Composites with a Refractory Dispersed Phase: Synthesis, Structure, and Application* (Ivan Fedorov, Tomsk, 2019) [in Russian].
69. M. A. Lagos, I. Agote, G. Atxaga, O. Adarraga, and L. Pambaguian, "Fabrication and Characterization of Titanium Matrix Composites Obtained Using a Combination of Self Propagating High Temperature Synthesis and Spark Plasma Sintering," Mater. Sci. Eng. A **655**, 44–49 (2016).
70. J. S. Kim et al., "Properties of Cu-Based Nanocomposites Produced by Mechanically-Activated Self-Propagating High-Temperature Synthesis and Spark-Plasma Sintering," J. Nanosci. Nanotechnol. **10**, 252–257 (2010).
71. D. V. Dudina, T. M. Vidyuk, M. A. Korchagin, A. I. Gavrilov, N. V. Bulina, M. A. Esikov, M. Datekyu, and H. Kato, "Interaction of a Ti–Cu Alloy with Carbon: Synthesis of Composites and Model Experiments," Materials **12** (9), Article number 1482 (2019).